

Proteomic Profiling of Accessory Structures from the Mouse Sperm Flagellum*[§]

Wenlei Cao, George L. Gerton[‡], and Stuart B. Moss^{‡§}

The flagellum of a mammalian spermatozoon consists of an axoneme surrounded in distinct regions by accessory structures known as the fibrous sheath, outer dense fibers, and the mitochondrial sheath. Although the characterization of individual proteins has provided clues about the roles of these accessory structures, a more complete understanding of flagellar function requires the identification of all the polypeptides in these assemblies. Epididymal mouse sperm were treated with SDS to dislodge sperm heads and to extract the axoneme and membranous elements. The remaining flagellar accessory structures were purified by sucrose gradient centrifugation. Analysis of proteins from these structures by two-dimensional gel electrophoresis and colloidal Coomassie Blue staining showed a highly reproducible pattern of >200 spots. Individual spots were picked, digested with trypsin, and identified by mass spectrometry and peptide microsequencing. Approximately 50 individual proteins were identified that could be assigned to five general categories: 1) proteins previously reported to localize to the accessory structures, e.g. ODF2 in the outer dense fibers, the sperm-specific glyceraldehyde-3-phosphate dehydrogenase in the fibrous sheath, and glutathione peroxidase in the mitochondrial sheath, validating this proteomic approach; 2) proteins that had not been shown to localize to any accessory structure but would be predicted to be present, e.g. glycolytic enzymes; 3) proteins known to be part of the flagellum but not localized to a specific site, e.g. adenylate kinase; 4) proteins not expected to be part of the accessory structures based on their previously reported locations, e.g. tektins; and 5) unknown proteins for which no information is available to make a determination as to location. The unexpected presence of the tektins in the accessory structures of the flagellum was confirmed by both immunoblot and immunofluorescence analysis. This proteomic analysis identified a number of unexpected and novel proteins in the accessory structures of the mammalian flagellum. *Molecular & Cellular Proteomics* 5:801–810, 2006.

The mammalian sperm flagellum is a complex structure whose proper assembly and function are critical for sperm

From the Center for Research on Reproduction and Women's Health, University of Pennsylvania School of Medicine, Philadelphia, Pennsylvania 19104

Received, September 30, 2005, and in revised form, January 23, 2006

Published, MCP Papers in Press, January 31, 2006, DOI 10.1074/mcp.M500322-MCP200

motility and subsequent fertilization of the egg. Morphologically the flagellum is characterized by three distinct regions: the midpiece, the principal piece, and the end piece. Common to these three segments is the axoneme or "motor" of the flagellum that runs the length of this structure and is composed of the typical "9 + 2" array of microtubules (1, 2). In the different segments, the axoneme may be surrounded by accessory structures: the mitochondrial sheath, outer dense fibers (ODFs),¹ and/or the fibrous sheath (FS). The midpiece is proximal to the sperm head and contains nine ODFs paired with the nine peripheral doublet microtubules, forming a "9 + 9 + 2" pattern. The mitochondrial sheath contains all the mitochondria of the sperm and is helically arranged around the ODFs in this region. Proximal to the midpiece is the principal piece. Seven of the nine ODFs extend through the principal piece, but fibers 3 and 8 are replaced by the longitudinal columns of the FS that are connected by numerous regularly spaced circumferential ribs. The FS underlies the plasma membrane and encases the ODFs and axoneme. Toward the distal end of the principal piece, the ODFs and FS taper off and terminate. The remaining short segment is the end piece that consists of the axoneme surrounded by the plasma membrane. Although the 9 + 2 arrangement of the axoneme is similar to other ciliary structures, the ODFs and FS are unique to sperm flagella.

Numerous genetic and proteomic studies of cilia have elucidated the primary structure of axonemal proteins, leading to a better understanding of their function (3, 4); however, less attention has been paid to the accessory structures unique to sperm flagella. Each structure is composed of a heterogeneous array of polypeptides, but relatively few of these have been identified and characterized (5–9). The ODF, FS, and mitochondrial sheath proteins that have been identified are conserved among various mammalian species, suggesting they perform critical functions. Although the identification of specific proteins has not been particularly informative as to the function(s) of the ODFs, the characterization of FS proteins has been more revealing. In addition to being a structural entity that provides a support for the flagellum, FS proteins are involved in cellular signaling and metabolism (5, 10).

¹ The abbreviations used are: ODF, outer dense fiber; FS, fibrous sheath; 1D, one-dimensional; 2D, two-dimensional; AK, adenylate kinase; AKAP, A-kinase anchor protein; PKA, cAMP-dependent protein kinase A; GAPD-S, sperm-specific isoform of glyceraldehyde-3-phosphate dehydrogenase.

Recognizing that only a few flagellar accessory structure proteins have been characterized at the molecular level, we hypothesized that the identification of additional ODF, FS, and mitochondrial sheath components would provide a better understanding of their function. Taking advantage of the SDS-insoluble nature of the accessory structures to isolate them free of axonemal and plasma membrane components, we utilized two-dimensional gel electrophoresis and mass spectrometry to identify >50 proteins present in these structures. These findings support a role for these structures in cell signaling, glycolysis, and metabolism during sperm function.

EXPERIMENTAL PROCEDURES

Sperm Preparation—Epididymal sperm were collected from male mice (CD1 retired breeders, Charles River Laboratories, Wilmington, MA) by mincing the caudae epididymides and allowing the sperm to swim out in PBS. The sperm were collected by centrifugation at $800 \times g$ for 5 min at room temperature, and SDS-resistant head and tail structures were isolated (11). Briefly sperm were homogenized in 1% SDS, 75 mM NaCl, 24 mM EDTA, pH 6.0 (S-EDTA); layered on 1.6 M sucrose gradient in S-EDTA; and centrifuged at $5000 \times g$ for 1 h at room temperature. The SDS-resistant tail structures were collected from the interface. For one-dimensional (1D) gel electrophoresis, the sample was dissolved in SDS sample buffer (62.5 mM Tris-HCl, pH 6.8, 2% SDS, 100 mM DTT, 10% glycerol, 0.005% bromphenol blue) and boiled for 5 min. For two-dimensional (2D) gel electrophoresis, the sample was dissolved in 2D sample buffer (40 mM Tris-HCl, pH 9, 8 M urea, 4% (w/v) CHAPS, 100 mM DTT, $1 \times$ protease inhibitor mixture (Roche Applied Science)). Samples for both 1D and 2D electrophoresis were centrifuged at $10,000 \times g$ for 5 min, and the pellet was discarded. The amount of protein was determined by the BCA method prior to 1D gel electrophoresis and the Bradford method prior to 2D gel electrophoresis (12, 13).

Gel Electrophoresis—Two-dimensional gel electrophoresis was performed with the Ettan IPGphor II and Ettan DALTsix equipment and PlusOne™ reagents from Amersham Biosciences. Samples (~100–900 μ g of protein in 200 μ l of sample buffer) were mixed with 250 μ l of rehydration buffer (8 M urea, 2% (w/v) CHAPS, 1% IPG buffer (pH 3–11, non-linear), 2 mg/ml DTT) and loaded in the IPGphor strip holder. Immobiline Drystrips (pH 3–11 non-linear, 24 cm) were placed in the holder and overlaid with ~4 ml of DryStrip cover fluid. Strips were hydrated under 50 V for 24 h and focused afterward on the IPGphor IEF system for a total of 80 kV-h at 20 °C.

After electrophoresis, each strip was equilibrated with 15 ml of equilibration buffer A (6 M urea, 100 mM Tris-HCl, pH 8.8, 30% (v/v) glycerol, 2% (w/v) SDS, 1% DTT) by rocking for 15 min and then with 15 ml of equilibration buffer B (6 M urea, 100 mM Tris-HCl, pH 8.8, 30% (v/v) glycerol, 2% (w/v) SDS, 2.5% iodoacetamide) for an additional 15 min. For the second dimension, the strips then were placed on top of 10% polyacrylamide gels containing SDS using the Ettan DALTsix apparatus. After electrophoresis, proteins were either stained with silver or with colloidal Coomassie Blue (for subsequent protein identification). The sizes of the proteins were estimated by comparing their positions with their theoretical molecular weights.

Mass Spectrometry and Microsequencing—Equipment and software were available in the Proteomics Core Facility at the University of Pennsylvania. Two-dimensional gels were scanned with a Typhoon 9400 scanner (Amersham Biosciences), and the spots were analyzed with Decyder software (Amersham Biosciences) and picked either manually or robotically. After digestion with trypsin, proteins were identified by MALDI-TOF/TOF mass spectrometry using a Voyager 4700 Proteomics Analyzer mass spectrometer (Applied Biosystems,

Foster City, CA). MALDI plates were calibrated using six calibration spots as recommended by the manufacturer, resulting in a mass accuracy of approximately ± 50 ppm. Peptide mass maps were acquired in reflectron mode (20-keV accelerating voltage) with 155-ns delayed extraction, averaging 2000 laser shots per spectrum. Trypsin autolytic peptides (m/z 842.51, 1045.56, and 2211.10) were used to internally calibrate each spectrum to a mass accuracy within 20 ppm. The MS/MS spectra were centroided and deisotoped using the AB 4700 controlling software based on a specified signal/noise ratio and the intensities of the fragment ions and then automatically stored by the AB 4700 controlling software. Additional filtering provided by the standard software package was in terms of the number of peaks per m/z region, which was set to the 20 most intense peaks per 200 Da. The mass range for fragment ions was always from 70 Da to the precursor mass minus 50 Da.

The spectra were analyzed using GPS Explorer (Version 3.0, Applied Biosystems), which acts as an interface between the Oracle database containing raw spectra and a local copy of the Mascot search engine (Version 1.9.05). Peptide peaks with a signal/noise ratio greater than 5 and a mass between m/z 900 and 4000 were searched against the National Center for Biotechnology Information (NCBI) Mouse Reference Sequence (RefSeq) database, release 5 (release date, May 02, 2004; number of accessions included, 1,255,613). The 10 most intense peaks were automatically selected for MS/MS. Up to one missed trypsin cut was allowed, and the data were searched using oxidation of methionine and carbamidomethylation of cysteine as variable modifications.

For microsequencing, peptide samples were dissolved in 5 μ l of 0.1% formic acid, injected into a C_{18} capillary column, and eluted by linearly increasing the mobile phase composition to 98% B (0.1% formic acid in 100% acetonitrile) at a flow rate of 200 nl/min. The eluted peptides were sequenced on line with a nanospray/Qstar-XL mass spectrometer (Applied Biosystems). The data were acquired and analyzed with Analyst QS. The protein identification and database search were performed with Mascot dll script of Analyst QS; the combined MS and MS/MS data were used for the Mascot database search. A protein score of >70 with a protein confidence of identification of >95% was considered acceptable.

Indirect Immunofluorescence Analyses—Epididymal sperm were collected, attached to slides, and fixed with 4% paraformaldehyde for 15 min. After washing with PBS, the sperm were permeabilized with -20 °C methanol for 2 min. The slides were washed with PBS, and the samples were incubated with 10% goat serum in PBS (blocking solution) for 30 min at room temperature and then with a rabbit anti-tektin antibody (generous gift of Dr. Christian Höög, 1:25 dilution) (14) in blocking solution for 1 h at room temperature. For a control, PBS-goat serum was substituted for the primary antibody. After washing with PBS, the samples were incubated with a secondary antibody linked with Fluo-488 (Molecular Probes, Eugene, OR) diluted 1:500 in blocking solution for 1 h at room temperature. After washing with PBS, the samples were mounted with coverslips using Fluoromount-G, examined using a Nikon Eclipse TE 300 microscope (Nikon Corp., Tokyo, Japan), and photographed with the MetaMorph® imaging system (Universal Imaging Corp., Downingtown, PA).

Immunoblot Analyses—Proteins from epididymal sperm and tail preparations were separated by SDS-PAGE on a 10% polyacrylamide gel and transferred to PVDF membranes (Millipore Corp., Bedford, MA). The membranes were blocked with TBST (25 mM Tris-HCl, pH 8.0, 125 mM NaCl, 0.1% Tween 20) containing 5% nonfat dry milk and incubated with either a mouse anti-bovine α -tubulin antibody (1:100 dilution) (Molecular Probes) or the rabbit anti-tektin antibody (1:100 dilution). After washing with TBST, the blots were incubated with either a goat anti-mouse IgG (to visualize tubulins) or a goat anti-rabbit IgG (to visualize tektins); both antibodies were conjugated to

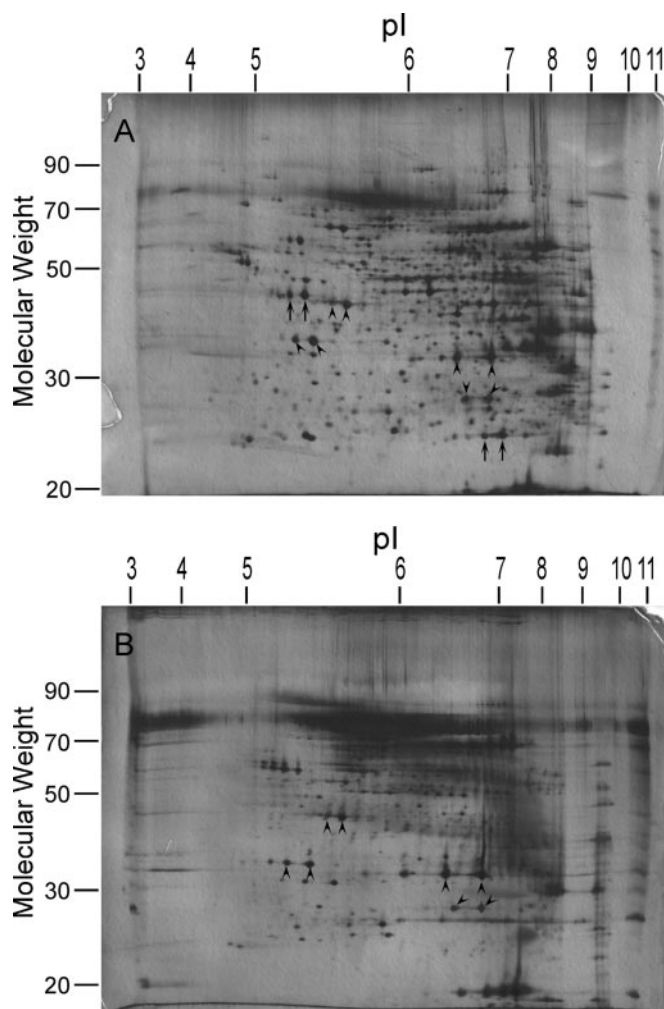


FIG. 1. Analytical 2D gel electrophoresis of whole sperm proteins (A) and SDS-resistant flagellar proteins (B) stained with silver. Some spots (arrows in A) were present only in the whole sperm sample, whereas others (arrowheads in both A and B) were present in both samples. Numbers along the top denote the pH gradient. Values on the left side represent approximate molecular weights.

horseradish peroxidase (Amersham Biosciences) and were used at a 1:5000 dilution. The bound enzyme was detected with the ECL kit (Amersham Biosciences) according to the manufacturer's directions and exposed to film.

RESULTS

Isolation of Accessory Structure Proteins and Separation by 2D Gel Electrophoresis—To isolate and identify proteins that comprise the accessory structures of the mammalian sperm flagellum, we prepared a particulate fraction containing SDS-resistant tail structures from epididymal sperm (15). As described previously, this tail fraction consists primarily of the accessory structures of the flagella (5). Although the axoneme and plasma membranes of the flagella are absent, the SDS-insoluble structures, *i.e.* the mitochondrial sheath, the ODF, and FS, still remain (schematic diagrams of whole sperm and of SDS-insoluble flagellar accessory structures are shown in

Fig. 5, I and J).

Both whole sperm and tail proteins were separated by 2D gel electrophoresis using a non-linear pH 3–11 gradient strip in the first dimension followed by SDS-PAGE in the second dimension. Multiple gels containing whole sperm proteins ($\sim 200 \mu\text{g}$) showed that, after silver staining, a highly reproducible pattern of protein spots was visualized (Fig. 1A). When SDS-insoluble tail proteins ($\sim 200 \mu\text{g}$) were analyzed, the pattern in multiple gels also was very reproducible (Fig. 1B). As expected, the patterns between the two protein samples were not identical. By comparison with whole sperm samples, we identified proteins that were absent in the tail preparations; these proteins represent components of the sperm head, axoneme, cytoplasm, or plasma membrane. Because high molecular weight proteins are difficult to detect by 2D gel electrophoresis, we were concerned that we would not be able to identify such polypeptides in the tail (16). However, after silver staining tail proteins separated by 1D SDS-PAGE, only one prominent band with $M_r > 90,000$ was observed, suggesting that we did not miss a large number of higher molecular weight proteins in our analysis.²

To identify proteins by mass spectrometry, the amount of SDS-insoluble tail proteins loaded for resolution by 2D gel electrophoresis was increased to $900 \mu\text{g}$, and the gel was stained with colloidal Coomassie Blue (Fig. 2A). When compared with a gel of tail proteins stained with silver (Fig. 1B), a similar, but not identical, protein pattern was observed. For example, a strong protein signal in the $M_r \sim 30,000$ – $40,000$ range was observed in the basic area (pH 7–9) of the gel (Fig. 2A, see proteins denoted 130, 131, and 132); the similar region in the silver-stained gel was less intense. The difference between the patterns of the two gels could be due to the stains used. The linear dynamic range of colloidal Coomassie Blue is 30–250 ng, whereas silver stain is not quantitative when amounts $> 60 \text{ ng}$ are present (17). In addition, silver stain shows more protein-to-protein variability, suggesting that some proteins may not be detected or may not appear to be as abundant as proteins stained with Coomassie. Variability in the detection of low abundance proteins by the two stains also may contribute to the differences in protein patterns. There also were two areas of the gel that did not resolve well presumably due to overloading, one at $M_r \sim 80,000$, pH 5.5–6.0 and one at $M_r \sim 30,000$, pH 7.0–9.0. To identify proteins in these regions, we decreased the amount of protein loaded to $100 \mu\text{g}$ (Fig. 2B).

Identification of Accessory Structure Proteins—The designated spots from gels shown in Fig. 2 were submitted to the proteomic core for analysis by MALDI-TOF/TOF mass spectrometry and microsequencing. Sequence information was obtained on more than 200 spots, and peptide matches to entries in the databases are shown (Supplemental Table 1). A few proteins were identified in multiple and diverse locations;

² W. Cao, G. L. Gerton, and S. B. Moss, unpublished observations.

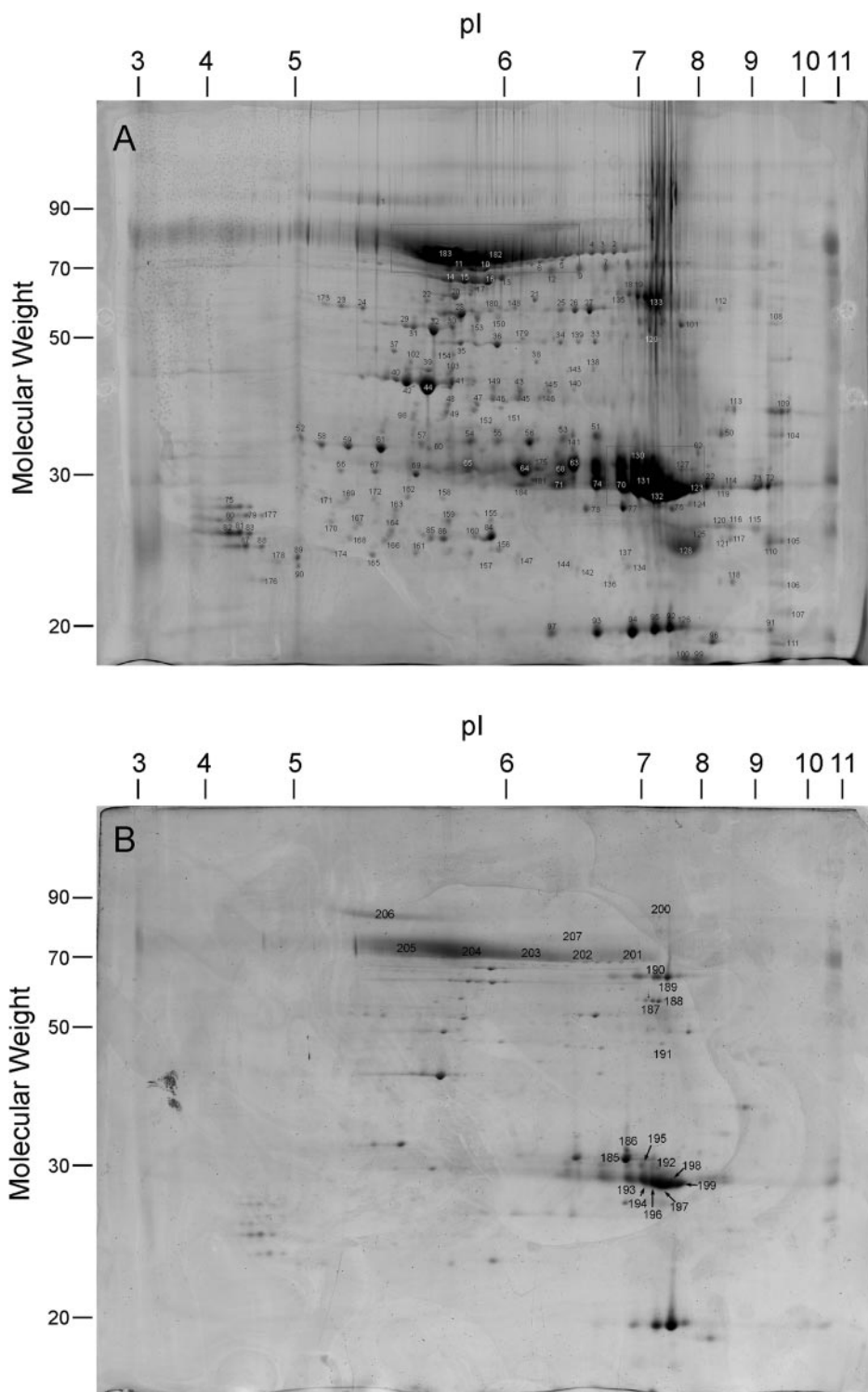


FIG. 2. Preparative 2D gel electrophoresis of SDS-resistant flagellar proteins stained with colloidal Coomassie Brilliant Blue. The gel in A contains ~900 μg of protein. The gel in B contains ~200 μg of protein and allowed the overloaded regions in A (rectangles) to be resolved. The numbered spots were picked and identified by MS and peptide microsequencing. Numbers along the top denote the pH gradient. Values on the left side represent approximate molecular weights.

this was particularly true for ODF2 (or ODF84). There were instances of multiple spots of the same protein that differed slightly by their pI, suggesting the presence of post-translational modifications (Fig. 2A, e.g. spots 92–95 represent glutathione peroxidase). Several spots contained peptides that corresponded to two proteins; however, one of these proteins

typically had a low “score” relative to the other. Some spots were not identified in this analysis. Many of the spots labeled “No ID” (e.g. spots 75, 79, 80, 81, 83, 87, and 88) were acidic proteins that probably do not have multiple cleavage sites for trypsin. Such digested peptides would be too long to be identified by MS. Other spots (e.g. spots 43 and 65) may not

TABLE I
Categorization of proteins from SDS-resistant structures of the sperm flagellum

Category/function	Protein	Known location in sperm	Spot no.	Sperm Refs.
1. Proteins previously localized to accessory structures Structural	ODF1	Outer dense fibers	51, 53–57, 60, 64, 68, 70–74, 123, 127, 130, 131, 175, 181, 184, 196–198	44, 45
	ODF2	Outer dense fibers	2–6, 14, 15, 20, 29–31, 39–42, 44–46, 48, 49, 85, 98, 102, 103, 134, 136, 137, 140, 142, 147–149, 151–154, 157, 158, 160–162, 164, 166–172, 180, 182, 183, 203, 204	7, 46
Oxidant defense	AKAP3	Fibrous sheath	1	18, 34
	AKAP4	Fibrous sheath	1	5, 47
	Sperm autoantigenic protein 17 (Sp17)	Fibrous sheath	176	48
	Glutathione S-transferase, Mu 5	Fibrous sheath	115, 116, 120	31
	Glutathione peroxidase 4	Mitochondrial sheath	91–95, 97, 126	21
Metabolism	Glyceraldehyde-3-phosphate dehydrogenase	Fibrous sheath	7–9, 12, 189, 190	8, 19
2. Proteins predicted to localize to accessory structures Structural	A-kinase anchoring protein-associated sperm protein	Not determined	156	49
Metabolism	Aldolase 1	Not determined	33, 139, 191	50
	Triose-phosphate isomerase	Not determined	52, 58, 59, 61, 66, 67, 69	50
	Phosphoglycerate kinase 2	Not determined	38	None
	Glycerol-3-phosphate dehydrogenase	Not determined	10, 11	51
3. Proteins known to part of the flagellum Metabolism	Adenylate kinase 1, cytosolic	AK activity in tail	165, 174	22
	Adenylate kinase 2, mitochondrial	AK activity in tail	77, 78	22
4. Proteins not expected to be part of accessory structures Structural	Tektin 1	Axoneme	37	None
	Tektin 2	Axoneme	35, 36	42
	Tektin 3	Axoneme	25–27	None
	Tektin 4 (RIKEN cDNA 1700010L19)	Axoneme	28	43
	Tektin 5 (RIKEN cDNA 3300001K11)	Not determined	18, 19	None
5. Unexpected proteins	Meiosis-specific nuclear structural protein 1	Not determined	17, 21	None
	Sperliolin (RIKEN cDNA 1700084J23)	Not determined	101, 108	26
	Sulfite oxidase	Not determined	22	None
	RAN guanine nucleotide release factor	Not determined	90	None
	Testis/prostate/placenta-expressed protein isoform 1	Not determined	105, 110, 117, 121	None
Asparaginase-like 1	Not determined	84, 86, 159	52	

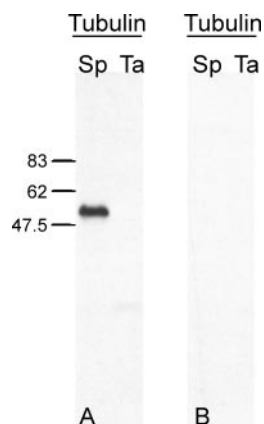


FIG. 3. Tubulin is not detected in proteins from the SDS-resistant flagellar preparation. A, immunoblot analysis of whole sperm proteins (Sp) and SDS-resistant flagellar proteins (Ta) with an anti- α -tubulin antibody. B, no primary antibody control.

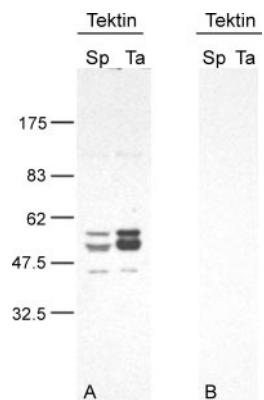


FIG. 4. Multiple tektins are present in proteins from the SDS-resistant flagellar preparation. A, immunoblot analysis of whole sperm proteins (Sp) and SDS-resistant flagellar proteins (Ta) with an anti-tektin antibody. B, no primary antibody control.

contain sufficient protein to be identified.

This analysis identified ~50 individual proteins that could be separated into five general categories: 1) proteins previously reported to localize to these structures, 2) proteins that had not been shown to localize to any accessory structures but would be predicted to be present, 3) proteins known to be part of the flagellum but not localized to a specific site, 4) proteins not expected to be part of the accessory structures based on their previously reported locations, and 5) unknown proteins for which information is not available to make a determination as to location or function (Table I). We did not find proteins associated with components of the sperm head, e.g. nucleus, perinuclear theca, and acrosome. Even though the tubulins are the most abundant proteins of the axoneme, neither α - nor β -tubulin was identified in the proteomic analysis. Furthermore α -tubulin was not detected by immunoblot analysis of SDS-insoluble tail proteins (Fig. 3).

Multiple Tektins Are Present in the Accessory Structures— The absence of tubulin in these tail preparations, combined

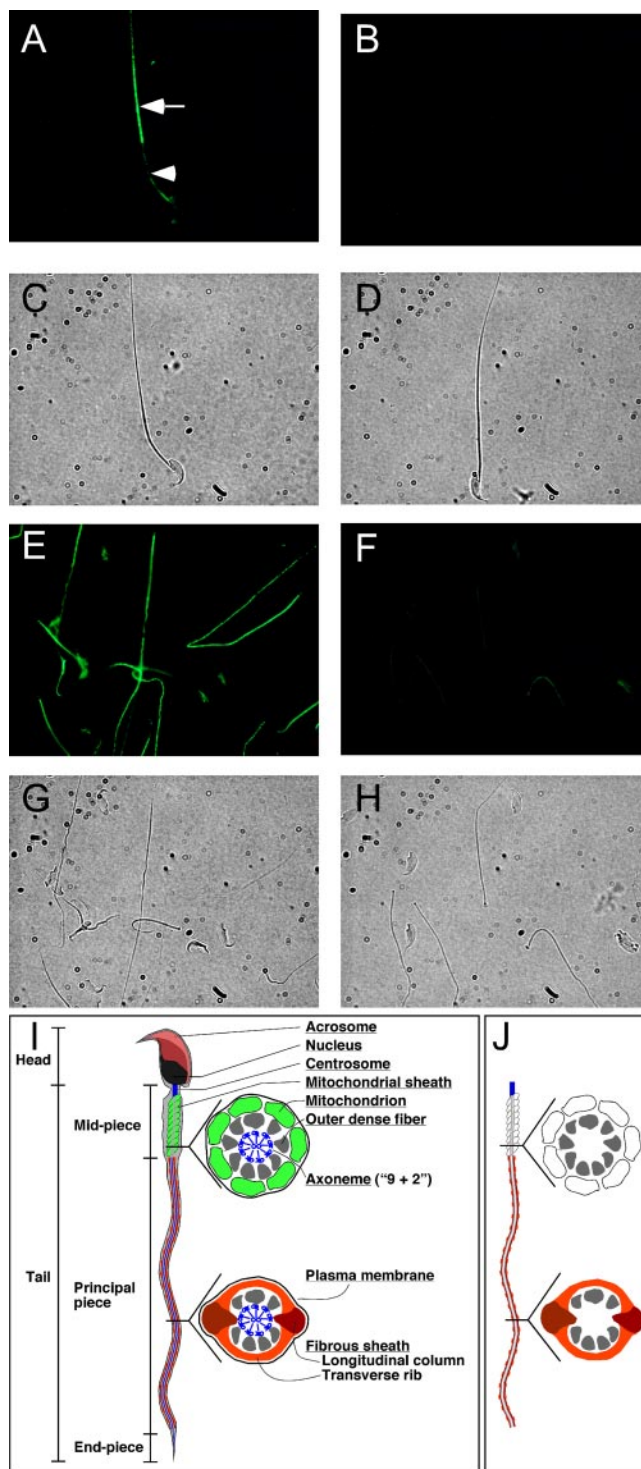


FIG. 5. Tektins are localized to the SDS-resistant flagellar structures. Whole sperm (A–D) and SDS-resistant flagellar structures (E–H) were prepared for immunofluorescence. A and E, cells incubated with an anti-tektin antibody. In A, the arrow denotes the principal piece, and the arrowhead denotes the midpiece of the sperm. C and G, corresponding brightfield images. B and F, flagellar structures incubated with secondary antibody alone. D and H, corresponding brightfield images. Magnification, 600 \times . I, schematic of whole sperm. J, schematic of SDS-insoluble flagellar accessory structures.

with transmission electron microscopy of the flagellar accessory structures (5), indicated that axonemal components were not present. As a consequence, we were surprised to identify multiple members of the tektin family; tektins 1, 2, and 3 and two mouse RIKEN clones (1700010L19 and 3300001K11) corresponding to novel tektins. The genes corresponding to these latter two clones have been designated *Tekt4* and *Tekt5*.³ To confirm the presence of these tektins in the accessory structures, proteins from both sperm and an SDS-insoluble tail preparation were separated by SDS-PAGE and probed with an antibody that recognizes multiple tektin isoforms (Fig. 4). Immunoreactive bands were detected in the sperm protein preparation at molecular weights consistent with those of tektins (M_r ~45,000–55,000). This immunoreactivity was even more predominant when SDS-insoluble tail proteins were analyzed. In addition, immunofluorescence of whole sperm detected tektins in the principal piece; however, SDS-insoluble tail preparations showed that tektins were present along the entire length of the flagellum (Fig. 5), suggesting that the tektins in the midpiece of intact sperm may not be accessible to the antibody.

DISCUSSION

The accessory structures, the FS, ODFs, and mitochondrial sheath, are unique to the sperm flagellum and are not found in cilia of other cells. We took advantage of the SDS-insoluble nature of these structures as a starting point for a proteomic analysis utilizing 2D gel electrophoresis and protein identification by mass spectrometry. From our proteomic analysis of the SDS-insoluble flagellar accessory structures, we analyzed >200 spots that represented ~50 individual proteins. These were placed into five different categories (Table I) and are discussed below.

Proteins Previously Reported to Localize to the Accessory Structures—The proteomic approach is validated by our identification of proteins that were shown previously to be in flagellar accessory structures. The protein kinase A anchor protein (AKAP), AKAP3, and the sperm-specific isoform of glyceraldehyde-3-phosphate dehydrogenase, GAPD-S, are present in the FS (8, 18, 19). We also identified ODF1 and ODF2, which are part of the outer dense fibers (7, 20). Glutathione peroxidase is found in mitochondria of the flagellar midpiece (21).

Of note from this analysis, many of the protein spots were identified as either ODF1 or ODF2. The identification of multiple forms of ODF proteins is not a new observation. For example, one-dimensional immunoblot analysis of ODF2 shows a very diverse pattern of polypeptides of M_r ~20,000–90,000 (7). There are several potential explanations for these observations. The multiple ODF1 or ODF2 spots could represent isoforms or post-translationally modified (e.g. phospho-

³ L. J. Maltais, The Jackson Laboratory, Bar Harbor, ME, personal communication.

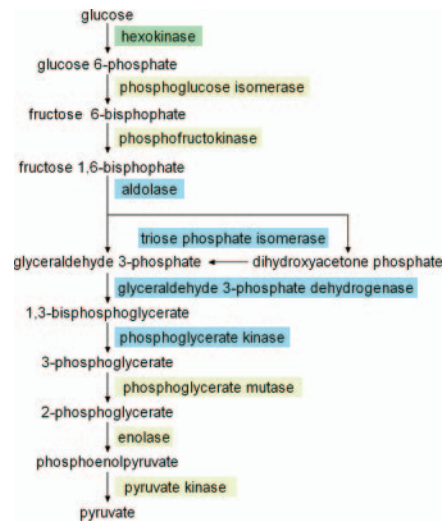


Fig. 6. **Enzymes of the glycolytic pathway are part of the SDS-insoluble tail.** Enzymes shaded in blue were identified in this study. Hexokinase (shaded in green) has been localized to the FS previously (6, 27). Aldolase cleaves fructose 1,6-bisphosphate to glyceraldehyde 3-phosphate and dihydroxyacetone phosphate.

rylated or proteolytically processed) versions of either protein. Alternatively these proteins might be particularly susceptible to degradation even though protease inhibitors were included in all steps of protein preparation and gel electrophoresis.

Proteins That Had Not Been Shown to Localize to Any Accessory Structure but Would be Predicted to be Present—Glycolytic enzymes, e.g. GAPD-S and the sperm-specific isoforms of hexokinase, HK1-sc, are localized to the FS where they are involved in ATP production. In this regard, the genetic ablation of GAPD-S results in the production of immotile sperm, implicating glycolysis as a critical source of energy for motility and suggesting that other glycolytic enzymes are tethered to the FS (10). We report in this study that aldolase 1, triose-phosphate isomerase, and phosphoglycerate kinase 2 were present in the SDS-insoluble tail preparation. As shown in Fig. 6, these findings indicate that the enzymes responsible for four consecutive steps in the glycolytic pathway (from the conversion of fructose 1,6-diphosphate to 3-phosphoglycerate) are localized to the accessory structures of the sperm flagellum. Because both HK1-sc and GAPD-S are part of the FS, we anticipate that aldolase, triose-phosphate isomerase, and phosphoglycerate kinase 2 also will be found tethered to this structure. Many of the remaining glycolytic enzymes are quite large (M_r >100,000), suggesting that they would not be detected by this type of 2D electrophoretic analysis. Nevertheless we predict that these enzymes will be localized to the principal piece and, perhaps, restricted to the FS. The assembly of the glycolytic components in the FS would create a “metabolosome” that could organize and coordinate the production of ATP in the sperm flagellum.

Proteins Known to Be Part of the Flagellum but Not Localized to a Specific Site—The demonstration that adenylate

kinases (AK1 and AK2) (ATP:AMP phosphotransferase) are present in the accessory structure(s) is intriguing. Schoff *et al.* (22) previously showed that AK activity exists in flagella and can generate sufficient ATP to produce normal motility in digitonin-permeabilized bovine sperm treated with 0.5 mM MgADP. Furthermore P^1, P^5 -di(adenosine 5')-pentaphosphate (Ap_5A), an adenylate kinase-specific inhibitor, blocks AK activity and sperm motility. Based on analogy to somatic cells, we predict that the two isoforms identified in our study have different localizations, *i.e.* AK2 is in the sperm mitochondria, whereas the “cytoplasmic” AK1 is associated with the FS and/or ODFs. Experiments to verify these predictions are in progress. The localization of AK to flagellar accessory structures of mammalian sperm (this study) and trypanosomes (paraflagellar rod) (23) suggests that a common mechanism exists for the generation of ATP in these structures.

Proteins Known to Be Part of the Flagellum but Not Expected to Be Part of the Accessory Structures—The tektins are constitutive proteins of microtubules in cilia, flagella, basal bodies, and centrioles and are thought to play a role in the stability of axonemal microtubules. They comprise one of the protofilaments in the wall of the A tubule and have different extraction properties compared with doublet microtubules (24). We discovered and confirmed by immunoblot and immunofluorescence analysis that five members of the tektin family, tektins 1–3 and the newly identified tektins 4 and 5, are part of the tail structures that are insoluble in SDS.

Additional Proteins Found in the Flagellar Accessory Structures—Two additional classes of proteins were identified in the SDS-insoluble tail fraction. One class consists of previously uncharacterized proteins. The second class includes proteins that have already been described, but their discovery in sperm flagellar structures was unexpected. For example, the meiosis-specific nuclear structural protein 1 is a skeletal protein that has been proposed to be nuclear and/or perinuclear during meiotic prophase (25). Another protein, speriolin (RIKEN cDNA 1700084J23), recently was identified and characterized by its ability to interact with Cdc20 (26). Speriolin associates with centrosomes during meiosis and then is found in the cytoplasm of condensing spermatids; although present in sperm, its location was not reported. As we found for sperm, both meiosis-specific nuclear structural protein 1 and speriolin are detergent-resistant proteins in spermatids. The presence of these proteins in flagellar structures suggests that they may have additional functions in sperm.

Known Flagellar Accessory Proteins Not Found in This Analysis—Although the identification of a number of proteins known to be part of the accessory structures of the sperm flagellum verified this proteomic approach, some proteins that we predicted to be found were not. Many of these polypeptides, *e.g.* glycolytic enzymes, have molecular weights >100,000, a size that does not resolve well by 2D gel electrophoresis. For example, HK1-sc (M_r ~116,000) was not found even though it is present in both the midpiece and

principal piece (6, 27). Furthermore HK1-sc is not tightly tethered to the FS, suggesting that it was extracted during the preparation of the tail structures (28).

We also expected that AKAP4 (M_r ~82,000), the major protein of the FS, would have been more readily detected. However, our procedure was to isolate discrete spots following 2D gel electrophoresis. Mouse AKAP4, on the other hand, tends to migrate as a broad smear under these conditions.² This may be an inherent solubility property of AKAP4 and reflect the phosphorylation status of the protein (29).

Implications—We identified ~50 proteins as being part of the SDS-insoluble flagellar structures. Previous investigators considered the FS and ODFs as structures that modulate flagellar bending in motile sperm (1, 30). However, with the identification of polypeptides that comprise these structures, it is becoming clear that they are also dynamic entities, having roles in signaling, metabolism, and oxidative stress (5, 10, 31). We initially identified AKAP4, the major FS component, as a scaffolding protein by its ability to bind the regulatory subunit of the cAMP-dependent protein kinase A (PKA) (5). Because sperm motility is regulated by a series of protein phosphorylation/dephosphorylation events, the tethering of PKA to a specific subdomain of the flagellum suggests that AKAP4 is involved in the cAMP regulation of motility. The subsequent identification of other AKAPs in the FS and mitochondrial sheath indicates that the scaffolding of proteins may be a common mechanism in the highly compartmentalized spermatozoon (18, 32–34). In addition, proteins other than PKA have been shown to bind these sperm AKAPs (35, 36). These findings have caused a reassessment of our previous concepts of multicomponent signal transduction systems. The assembly of signaling molecules into macromolecular complexes, *i.e.* “transducisomes” or “signalosomes” may provide specificity, sensitivity, and speed in intracellular signaling pathways.

Many of the proteins from the SDS-insoluble tail structures are involved in the generation and utilization of ATP. Glycolysis occurs in the FS to generate ATP utilized both by PKA to regulate motility as well as by the dynein ATPases, which function as the flagellar motors. We identified the voltage-dependent anion channel 2 as part of our proteomic analysis, a finding consistent with its known presence in ODFs (37). The ability of the voltage-dependent anion channel 2 protein to bind and transport ATP has led to the hypothesis that their presence in the ODFs is important for the trafficking of ATP along the flagellum (37). Another mechanism to ensure availability of ATP is the reaction catalyzed by adenylate kinase that can generate one molecule each of ATP and AMP from two molecules of ADP. Mammalian sperm do not have the components of a phosphocreatine shuttle system as found in the sea urchin that allows the transport of high energy phosphate from the mitochondria to the axoneme (38). Instead of diffusion of ATP from mitochondria, energy for sperm motility is generated in the FS by glycolysis (10). AK can produce

either ADP or stoichiometric amounts of ATP and AMP depending on the concentrations of the three nucleotides. In locations where ATP is utilized rapidly, e.g. the sperm flagellum, the direction favors the production of one molecule each of ATP and AMP from two molecules of ADP.

AK activity and tektins have been reported in cilia and flagella from a number of organisms (22, 23, 39, 40). Our proteomic analysis identified AK and tektins in the detergent-insoluble structures, which lack the axoneme. In *Chlamydomonas*, whose flagella do not contain the accessory structures typical of mammalian sperm, AK is found in association with the outer dynein arm-docking complex (41). This assembly is part of the A tubule of the outer microtubular doublets of the axoneme. Similarly the tektins also are localized to the walls of the A tubule; specifically they are near the binding site for the radial spokes, inner dynein arms, and nexin links (24). The genetic ablation of tektin-t (tektin 2) results in immotile sperm that show defects in dynein inner arm structure, suggesting that this tektin participates in inner arm formation and attachment (42). Tektin 4 also has been reported in flagella of rat sperm (43). Based on the identification of both AKs and tektins as part of the SDS-insoluble tail, we would predict that these proteins form a tight association with the ODFs as part of the 9 + 9 + 2 axonemal ODF organization. We are currently examining whether these proteins are involved in linking the axoneme to the accessory structures.

This study, along with previous investigations, demonstrates that the flagellar accessory structures are more than passive cytoskeletal elements. The presence of metabolic and signaling proteins indicates that the FS, mitochondrial sheath, and ODFs have active roles in sperm physiology. A knowledge of the assembly and activities of these structures may open up new avenues for understanding the basis for male reproduction.

Acknowledgments—Mass spectrometry and peptide microsequencing were provided by the Proteomics Core Facility of the Genomics Institute and the Abramson Cancer Center at the University of Pennsylvania. We thank Dr. Chao-Xing Yuan and Christine Busch of this facility for expertise and guidance during the course of this work. We thank Dr. Christian Höög (Stockholm, Sweden) for the generous gift of the anti-tektin antibody.

* This work was supported by National Institutes of Health Grant HD06427. The costs of publication of this article were defrayed in part by the payment of page charges. This article must therefore be hereby marked "advertisement" in accordance with 18 U.S.C. Section 1734 solely to indicate this fact.

§ The on-line version of this article (available at <http://www.mcponline.org>) contains supplemental material.

‡ Co-principal investigators.

§ To whom correspondence should be addressed: Center for Research on Reproduction and Women's Health, 1312 BRB II, 421 Curie Blvd., University of Pennsylvania Medical School, Philadelphia, PA 19104. Tel.: 215-573-4782; Fax: 215-573-7627; E-mail: smoss@mail.med.upenn.edu.

REFERENCES

- Fawcett, D. W. (1975) The mammalian spermatozoon. *Dev. Biol.* **44**, 394–436
- Oko, R., and Clermont, Y. (1990) Mammalian spermatozoa: structure and assembly of the tail, in *Controls of Sperm Motility: Biological and Clinical Aspects* (Gagnon, C., ed) pp. 3–27. CRC Press, Boca Raton, FL
- Li, J. B., Gerdes, J. M., Haycraft, C. J., Fan, Y., Teslovich, T. M., May-Simera, H., Li, H., Blacque, O. E., Li, L., Leitch, C. C., Lewis, R. A., Green, J. S., Parfrey, P. S., Leroux, M. R., Davidson, W. S., Beales, P. L., Guay-Woodford, L. M., Yoder, B. K., Stormo, G. D., Katsanis, N., and Dutcher, S. K. (2004) Comparative genomics identifies a flagellar and basal body proteome that includes the BBS5 human disease gene. *Cell* **117**, 541–552
- Ostrowski, L. E., Blackburn, K., Radde, K. M., Moyer, M. B., Schlatter, D. M., Moseley, A., and Boucher, R. C. (2002) A proteomic analysis of human cilia: identification of novel components. *Mol. Cell. Proteomics* **1**, 451–465
- Carrera, A., Gerton, G. L., and Moss, S. B. (1994) The major fibrous sheath polypeptide of mouse sperm: structural and functional similarities to the A-kinase anchoring proteins. *Dev. Biol.* **165**, 272–284
- Travis, A. J., Foster, J. A., Rosenbaum, N. A., Visconti, P. E., Gerton, G. L., Kopf, G. S., and Moss, S. B. (1998) Targeting of a germ cell-specific type 1 hexokinase lacking a porin-binding domain to the mitochondria as well as to the head and fibrous sheath of murine spermatozoa. *Mol. Biol. Cell* **9**, 263–276
- Schalles, U., Shao, X., van der Hoorn, F. A., and Oko, R. (1998) Developmental expression of the 84-kDa ODF sperm protein: localization to both the cortex and medulla of outer dense fibers and to the connecting piece. *Dev. Biol.* **199**, 250–260
- Bunch, D. O., Welch, J. E., Magyar, P. L., Eddy, E. M., and O'Brien, D. A. (1998) Glyceraldehyde 3-phosphate dehydrogenase-S protein distribution during mouse spermatogenesis. *Biol. Reprod.* **58**, 834–841
- Bhullar, B., Zhang, Y., Junco, A., Oko, R., and van der Hoorn, F. A. (2003) Association of kinesin light chain with outer dense fibers in a microtubule-independent fashion. *J. Biol. Chem.* **278**, 16159–16168
- Miki, K., Qu, W., Goulding, E. H., Willis, W. D., Bunch, D. O., Strader, L. F., Perreault, S. D., Eddy, E. M., and O'Brien, D. A. (2004) Glyceraldehyde 3-phosphate dehydrogenase-S, a sperm-specific glycolytic enzyme, is required for sperm motility and male fertility. *Proc. Natl. Acad. Sci. U. S. A.* **101**, 16501–16506
- O'Brien, D. A., and Bellve, A. R. (1980) Protein constituents of the mouse spermatozoon. II. Temporal synthesis during spermatogenesis. *Dev. Biol.* **75**, 405–418
- Bradford, M. M. (1976) A rapid and sensitive method for the quantitation of microgram quantities of protein utilizing the principle of protein-dye binding. *Anal. Biochem.* **72**, 248–254
- Smith, P. K., Krohn, R. I., Hermanson, G. T., Mallia, A. K., Gartner, F. H., Provenzano, M. D., Fujimoto, E. K., Goeke, N. M., Olson, B. J., and Klenk, D. C. (1985) Measurement of protein using bicinchoninic acid. *Anal. Biochem.* **150**, 76–85
- Larsson, M., Norrander, J., Graslund, S., Brundell, E., Linck, R., Stahl, S., and Hoog, C. (2000) The spatial and temporal expression of Tekt1, a mouse tektin C homologue, during spermatogenesis suggest that it is involved in the development of the sperm tail basal body and axoneme. *Eur. J. Cell Biol.* **79**, 718–725
- O'Brien, D. A., and Bellve, A. R. (1980) Protein constituents of the mouse spermatozoon. I. An electrophoretic characterization. *Dev. Biol.* **75**, 386–404
- Olivieri, E., Herbert, B., and Righetti, P. G. (2001) The effect of protease inhibitors on the two-dimensional electrophoresis pattern of red blood cell membranes. *Electrophoresis* **22**, 560–565
- Berggren, K., Chernokalskaya, E., Steinberg, T. H., Kemper, C., Lopez, M. F., Diwu, Z., Haugland, R. P., and Patton, W. F. (2000) Background-free, high sensitivity staining of proteins in one- and two-dimensional sodium dodecyl sulfate-polyacrylamide gels using a luminescent ruthenium complex. *Electrophoresis* **21**, 2509–2521
- Mandal, A., Naaby-Hansen, S., Wolkowicz, M. J., Klotz, K., Shetty, J., Retief, J. D., Coonrod, S. A., Kinter, M., Sherman, N., Cesar, F., Flickinger, C. J., and Herr, J. C. (1999) FSP95, a testis-specific 95-kilodalton fibrous sheath antigen that undergoes tyrosine phosphorylation in capacitated human spermatozoa. *Biol. Reprod.* **61**, 1184–1197

19. Westhoff, D., and Kamp, G. (1997) Glyceraldehyde 3-phosphate dehydrogenase is bound to the fibrous sheath of mammalian spermatozoa. *J. Cell Sci.* **110**, 1821–1829
20. Morales, C. R., Alcivar, A. A., Hecht, N. B., and Griswold, M. D. (1989) Specific mRNAs in Sertoli and germinal cells of testes from stage synchronized rats. *Mol. Endocrinol.* **3**, 725–733
21. Godeas, C., Tramer, F., Micali, F., Soranzo, M., Sandri, G., and Panfili, E. (1997) Distribution and possible novel role of phospholipid hydroperoxide glutathione peroxidase in rat epididymal spermatozoa. *Biol. Reprod.* **57**, 1502–1508
22. Schoff, P. K., Cheetham, J., and Lardy, H. A. (1989) Adenylate kinase activity in ejaculated bovine sperm flagella. *J. Biol. Chem.* **264**, 6086–6091
23. Pullen, T. J., Ginger, M. L., Gaskell, S. J., and Gull, K. (2004) Protein targeting of an unusual, evolutionarily conserved adenylate kinase to a eukaryotic flagellum. *Mol. Biol. Cell* **15**, 3257–3265
24. Nojima, D., Linck, R. W., and Egelman, E. H. (1995) At least one of the protofilaments in flagellar microtubules is not composed of tubulin. *Curr. Biol.* **5**, 158–167
25. Furukawa, K., Inagaki, H., Naruge, T., Tabata, S., Tomida, T., Yamaguchi, A., Yoshikuni, M., Nagahama, Y., and Hotta, Y. (1994) cDNA cloning and functional characterization of a meiosis-specific protein (MNS1) with apparent nuclear association. *Chromosome Res.* **2**, 99–113
26. Goto, M., and Eddy, E. M. (2004) Speriolin is a novel spermatogenic cell-specific centrosomal protein associated with the seventh WD motif of Cdc20. *J. Biol. Chem.* **279**, 42128–42138
27. Mori, C., Nakamura, N., Welch, J. E., Gotoh, H., Goulding, E. H., Fujioka, M., and Eddy, E. M. (1998) Mouse spermatogenic cell-specific type 1 hexokinase (mHk1-s) transcripts are expressed by alternative splicing from the mHk1 gene and the HK1-S protein is localized mainly in the sperm tail. *Mol. Reprod. Dev.* **49**, 374–385
28. Travis, A. J., Jorgez, C. J., Merdiushev, T., Jones, B. H., Dess, D. M., Diaz-Cueto, L., Storey, B. T., Kopf, G. S., and Moss, S. B. (2001) Functional relationships between capacitation-dependent cell signaling and compartmentalized metabolic pathways in murine spermatozoa. *J. Biol. Chem.* **276**, 7630–7636
29. Ficarro, S., Chertihin, O., Westbrook, V. A., White, F., Jayes, F., Kalab, P., Marto, J. A., Shabanowitz, J., Herr, J. C., Hunt, D. F., and Viscconti, P. E. (2003) Phosphoproteome analysis of capacitated human sperm. Evidence of tyrosine phosphorylation of a kinase-anchoring protein 3 and valosin-containing protein/p97 during capacitation. *J. Biol. Chem.* **278**, 11579–11589
30. Lindemann, C. B., Orlando, A., and Kanous, K. S. (1992) The flagellar beat of rat sperm is organized by the interaction of two functionally distinct populations of dynein bridges with a stable central axonemal partition. *J. Cell Sci.* **102**, 249–260
31. Fulcher, K. D., Welch, J. E., Klapper, D. G., O'Brien, D. A., and Eddy, E. M. (1995) Identification of a unique mu-class glutathione S-transferase in mouse spermatogenic cells. *Mol. Reprod. Dev.* **42**, 415–424
32. Lin, R. Y., Moss, S. B., and Rubin, C. S. (1995) Characterization of S-AKAP84, a novel developmentally regulated A kinase anchor protein of male germ cells. *J. Biol. Chem.* **270**, 27804
33. Mei, X., Singh, I. S., Erlichman, J., and Orr, G. A. (1997) Cloning and characterization of a testis-specific, developmentally regulated A-kinase-anchoring protein (TAKAP-80) present on the fibrous sheath of rat sperm. *Eur. J. Biochem.* **246**, 425–432
34. Vijayaraghavan, S., Liberty, G. A., Mohan, J., Winfrey, V. P., Olson, G. E., and Carr, D. W. (1999) Isolation and molecular characterization of AKAP110, a novel, sperm-specific protein kinase A-anchoring protein. *Mol. Endocrinol.* **13**, 705–717
35. Carr, D. W., Fujita, A., Stentz, C. L., Liberty, G. A., Olson, G. E., and Narumiya, S. (2001) Identification of sperm-specific proteins that interact with A-kinase anchoring proteins in a manner similar to the type II regulatory subunit of PKA. *J. Biol. Chem.* **276**, 17332–17338
36. Brown, P. R., Miki, K., Harper, D. B., and Eddy, E. M. (2003) A-kinase anchoring protein 4 binding proteins in the fibrous sheath of the sperm flagellum. *Biol. Reprod.* **68**, 2241–2248
37. Hinsch, K. D., De Pinto, V., Aires, V. A., Schneider, X., Messina, A., and Hinsch, E. (2004) Voltage-dependent anion-selective channels VDAC2 and VDAC3 are abundant proteins in bovine outer dense fibers, a cytoskeletal component of the sperm flagellum. *J. Biol. Chem.* **279**, 15281–15288
38. Tombes, R. M., and Shapiro, B. M. (1985) Metabolite channeling: a phosphorylcreatine shuttle to mediate high energy phosphate transport between sperm mitochondrion and tail. *Cell* **41**, 325–334
39. Hastie, A., Colizzo, F., Evans, L., Krantz, M., and Fish, J. (1992) Initial characterization of tektins in cilia of respiratory epithelial cells. *Chest* **101**, 47S–48S
40. Ota, A., Kusakabe, T., Sugimoto, Y., Takahashi, M., Nakajima, Y., Kawaguchi, Y., and Koga, K. (2002) Cloning and characterization of testis-specific tektin in Bombyx mori. *Comp. Biochem. Physiol. B Biochem. Mol. Biol.* **133**, 371–382
41. Wirschell, M., Pazour, G., Yoda, A., Hirono, M., Kamiya, R., and Witman, G. B. (2004) Oda5p, a novel axonemal protein required for assembly of the outer dynein arm and an associated adenylate kinase. *Mol. Biol. Cell* **15**, 2729–2741
42. Tanaka, H., Iguchi, N., Toyama, Y., Kitamura, K., Takahashi, T., Kaseda, K., Maekawa, M., and Nishimune, Y. (2004) Mice deficient in the axonemal protein Tektin-t exhibit male infertility and immotile-cilium syndrome due to impaired inner arm dynein function. *Mol. Cell. Biol.* **24**, 7958–7964
43. Matsuyama, T., Honda, Y., Doiguchi, M., and Iida, H. (2005) Molecular cloning of a new member of TEKTIN family, Tektin4, located to the flagella of rat spermatozoa. *Mol. Reprod. Dev.* **72**, 120–128
44. Higgy, N. A., Pastoor, T., Renz, C., Tarnasky, H. A., and Van der Hoorn, F. A. (1994) Testis-specific RT7 protein localizes to the sperm tail and associates with itself. *Biol. Reprod.* **50**, 1357–1366
45. Brohmann, H., Pinnecke, S., and Hoyer-Fender, S. (1997) Identification and characterization of new cDNAs encoding outer dense fiber proteins of rat sperm. *J. Biol. Chem.* **272**, 10327–10332
46. Hoyer-Fender, S., Petersen, C., Brohmann, H., Rhee, K., and Wolgemuth, D. J. (1998) Mouse Odf2 cDNAs consist of evolutionary conserved as well as highly variable sequences and encode outer dense fiber proteins of the sperm tail. *Mol. Reprod. Dev.* **51**, 167–175
47. Fulcher, K. D., Mori, C., Welch, J. E., O'Brien, D. A., Klapper, D. G., and Eddy, E. M. (1995) Characterization of Fsc1 cDNA for a mouse sperm fibrous sheath component. *Biol. Reprod.* **52**, 41–49
48. Lea, I. A., Widgren, E. E., and O'Rand, M. G. (2004) Association of sperm protein 17 with A-kinase anchoring protein 3 in flagella. *Biol. Endocrinol.* **2**, 57
49. Anway, M. D., Ravindranath, N., Dym, M., and Griswold, M. D. (2002) Identification of a murine testis complementary DNA encoding a homolog to human A-kinase anchoring protein-associated sperm protein. *Biol. Reprod.* **66**, 1755–1761
50. Storey, B. T., and Kayne, F. J. (1975) Energy metabolism of spermatozoa. V. The Embden-Myerhof pathway of glycolysis: activities of pathway enzymes in hypotonically treated rabbit epididymal spermatozoa. *Fertil. Steril.* **26**, 1257–1265
51. Jones, A. R., and Gillan, L. (1996) Glycerol 3-phosphate dehydrogenase of boar spermatozoa: inhibition by α -bromohydrin phosphate. *J. Reprod. Fertil.* **108**, 95–100
52. Bush, L. A., Herr, J. C., Wolkowicz, M., Sherman, N. E., Shore, A., and Flickinger, C. J. (2002) A novel asparaginase-like protein is a sperm autoantigen in rats. *Mol. Reprod. Dev.* **62**, 233–247